

**A Unified Approach to Lane Change Intention Recognition and Driving Status  
Prediction through TCN-LSTM and Multi-Task Learning Models**

Renteng Yuan<sup>1,2</sup>

Graduate Research Assistant  
rtengyuan123@knights.ucf.edu

Mohamed Abdel-Aty<sup>2</sup>

Professor  
m.aty@ucf.edu

Xin Gu<sup>3</sup>

Lecturer  
guxin@bjut.edu.cn

Ou Zheng<sup>2</sup>

Research Scientist  
[ouzheng@knights.ucf.edu](mailto:ouzheng@knights.ucf.edu)

Qiaojun Xiang<sup>1\*</sup>

Professor  
[xqj@seu.edu.com](mailto:xqj@seu.edu.com)

1. Jiangsu Key Laboratory of Urban ITS, School of Transportation, Southeast University, Nanjing, Jiangsu, P. R. China, and 210000

2. Department of Civil, Environmental and Construction Engineering, University of Central Florida, 12800 Pegasus Dr #211, Orlando, FL 32816, USA

3. Beijing Key Laboratory of Traffic Engineering, Beijing University of Technology, Beijing, P. R. China, and 100124

\*Corresponding author

April 2023

**Abstract:**

Lane change (LC) is a continuous and complex operation process. Accurately detecting and predicting LC processes can help traffic participants better understand their surrounding environment, recognize potential LC safety hazards, and improve traffic safety. This present paper focuses on LC processes, developing an LC intention recognition (LC-IR) model and an LC status prediction (LC-SP) model. A novel ensemble temporal convolutional network with Long Short-Term Memory units (TCN-LSTM) is first proposed to capture long-range dependencies in sequential data. Then, three multi-task models (MTL-LSTM, MTL-TCN, MTL-TCN -LSTM) are developed to capture the intrinsic relationship among output indicators. Furthermore, a unified modeling framework for LC intention recognition and driving status prediction (LC-IR-SP) is developed. To validate the performance of the proposed models, a total number of 1023 vehicle trajectories is extracted from the CitySim dataset. The Pearson coefficient is employed to determine the related indicators. The results indicate that using 150 frames as input length, the TCN-LSTM model with 96.67% accuracy outperforms TCN and LSTM models in LC intention classification, and provides more balanced results for each class. Three proposed multi-tasking learning models provide markedly increased performance compared to corresponding single-task models, with an average reduction of 24.24% and 22.86% in the Mean Absolute Error (MAE) and Root Mean Square Error (RMSE), respectively. The developed LC-IR-SP model has promising applications for autonomous vehicles to identify lane change behaviors, calculate a real-time traffic conflict index and improve vehicle control strategies.

**Keywords:** lane-change recognition, driving status prediction, vehicle trajectory, multi-task learning, TCN-LSTM

## 1 Introduction

It can be expected that, for an extended period of time, vehicles with varying levels of automation will coexist on the roads, including those with human-driven and fully autonomous vehicles (Bagloee et al. 2016; Cabri et al. 2021). Assisting intelligent driving vehicles to understand and predict changes in the behavior of human-driven vehicles is particularly critical to ensure traffic safety during the transition period. Lane changing (LC) is a common driving behavior that leads to two-dimensional spatial (longitudinal and lateral) interaction between vehicles. The LC process consists of a series of continuous, complex maneuvering actions such as acceleration, deceleration, and steering, that have a significant impact on road traffic efficiency and safety (Chen et al. 2020a; Hou et al. 2015). Hence, accurately identifying the early lane change intention and predicting the future driving status of the lane change vehicle (e.g., speed, acceleration, driving direction, etc.) can effectively help intelligent driving vehicles or drivers anticipate potential safety risks and execute appropriate response strategies.

LC intention recognition has been a challenging problem in traffic engineering since it is hard to directly observe. There are two types of information that are typically utilized to identify LC intentions, vehicle dynamics indicators and driver characteristic indicators. Vehicle dynamics indicators include steering wheel angle, steering velocity, lateral velocity, turn signal, and brake pedal position (Guoqing et al. 2010; Kumar et al. 2013; Li et al. 2016; Liu and Pentland 1997). In addition to the difficulty of obtaining certain information directly from human-driven vehicles (e.g., steering wheel angle, steering velocity, etc.), the reliability of the data obtained is also difficult to guarantee. For example, turn signal usage is reported to be between 44% and 40% in the US and China, respectively (Li et al. 2016; Ruina et al. 2013). The driver characteristic indicators consist of head movement, eye movement, body gestures, and even electroencephalography (Doshi and Trivedi 2008; Gao et al. 2021; Gwon et al. 2017; McCall et al. 2007; Morris et al. 2011; Pan et al. 2022; Peng et al. 2020; Xing et al. 2020). Such information can only be gathered through sensors or driving simulation experiments. Inevitably, experimental settings constrain these investigations, such as potential concerns with low data quality, high cost, and small sample size, making it difficult to generalize and apply the research findings.

The driving status is characterized by factors such as the vehicle's velocity, acceleration, and driving direction. The research on driving status prediction can be classified into two categories: speed prediction (Cao et al. 2020; Yeon et al. 2019; Zhao et al. 2019a; Zhao et al. 2019b), and steering angle prediction (Gidado et al. 2020; Ijaz and Wang 2021; Jiang et al. 2020). However, previous modeling frameworks have required separate prediction models for each metric to predict the driving status, resulting in significant training time and potential conflicts between the prediction results of different metrics. In fact, these driving status indicators are interrelated, especially for vehicles that are changing lanes (Chen et al. 2015;

Yang et al. 2019). Considering the correlation among indicators, building a multi-task prediction model to predict multiple indicators simultaneously is necessary to reduce model training time and improve prediction performance (Ruder 2017).

With the advancement of technology, traffic system monitors and road users can obtain massive, real-time, individualized, and high-precision vehicle trajectory data. Vehicle trajectories are generated when the driver performs a series of driving maneuvers. Compared to complex driving maneuvers, vehicle trajectories are easier to observe and record. This paper focuses on the LC process, using vehicle trajectory data, and aims to build a unified approach to lane change intention recognition (LC-IR) and driving status prediction (LC-SP). The contribution of this paper is threefold.

- First, to overcome the limitations of LSTM and TCN networks, a novel ensemble temporal convolutional network with Long Short-Term Memory units (TCN-LSTM) is proposed to capture long-range dependencies in sequential data.

- Second, three multi-task learning models (MLT-LSTM, MLT-TCN, MLT-LSTM-TCN) are constructed and compared to predict driving status variables. To our knowledge, no studies simultaneously considered the intrinsic relationship between outcome factors to predict driving status indicators.

- Third, a new unified modeling framework for Lane Change Intention Recognition and Status Prediction (LC-IR -SP) based on vehicle trajectory data is proposed. A new vehicle trajectory dataset (CitySim Dataset) was employed to develop the LC-IR-SP modeling framework. As far as we know, this is the first study to combine lane change intention recognition and lane change status prediction.

The rest of this paper is structured as follows. Section 2 presents a brief literature review. The data collection and post-processing are described in Section 3. In Section 4, a novel ensemble temporal convolutional network with Long Short-Term Memory units (TCN-LSTM) and three multi-task models are proposed. The experimental results and discussion are included in Section 6, Section 7 draws out the conclusions of this study.

## **2 Literature review**

The LC behavior is a time-varying, continuous maneuvering process (Ali et al. 2022; Sheu and Ritchie 2001). There are three kinds of methods, including dynamic or kinematic models (Jo et al. 2012; Lefèvre et al. 2014; Li et al. 2022b; Polychronopoulos et al. 2007; Schmidt et al. 2014; Wang et al. 2014; Xu et al. 2012), statistical models (Guoqing et al. 2010; Kumar et al. 2013; McCall et al. 2007; Ng et al. 2020; Park et al. 2015; Wang et al. 2016), machine learning methods (Chen et al. 2020b; David and Söffker 2023; Gao et al. 2020; Izquierdo et al. 2019; Khelfa et al. 2023; Li et al. 2021; Mahajan et al. 2020), have been widely used for the LC intention recognition. The method based on dynamic or kinematic models detects the vehicle's motion by considering the kinematic relationship among

parameters (e.g. position, velocity, acceleration), and the different forces (the longitudinal and lateral tire forces, or the road banking angle) that affect the vehicle motions. As classical statistical methods, multinomial logit models and Bayesian theory are utilized to predict the lane change probability. To capture the inherent characteristics of time series, three machine learning methods, including Hidden Markov Model (HMM), Support Vector Machines (SVM), and Long Short-Term Memory (LSTM), have been widely used. The commonly used models and their performance are listed in Table 1.

Table 1 A summary of the representative research for LC intention recognition

Study	Method	Data	Number of Samples	Advance time	Accuracy
(Xu et al. 2021)	CNN	Image	637	--	73.97%
(Izquierdo et al. 2019)	GoogleNet & LSTM	Image	714	3.76s	74.46%
(Liu et al. 2022)	Vision-cloud data fusion	Image	-- (2 participants)	--	79.2%
(Guo et al. 2021)	AT-BiLSTM	Simulator	-- (25 participants)	3s	93.33%
(Guoqing et al. 2010)	BN	Simulator	-- (1 participants)	--	95.4%
(Zheng and Hansen 2017)	HMM	Naturalistic	-- (58 participants)	--	83.22%
(Kumar et al. 2013)	SVM	Naturalistic	139(6 participants)	1.3	80%
(Xing et al. 2020)	EBiLSTM	Naturalistic	201 (3participants)	0.5 s	96.1%
(Li et al. 2016)	HMM	Naturalistic	642(50 participants)	0.5s	90.3%
(Gao et al. 2020)	LSTM	Naturalistic	814(6 participants)	--	88.26%
(Doshi and Trivedi 2009)	RVM	Naturalistic	903(8 participants)	3s	88.51%
(Zheng et al. 2014)	NN	Trajectory	Above 1000	--	73.33%
(Wang et al. 2022)	LSTM	Trajectory	---	2.5s.	92.40 %
(Ng et al. 2020)	Logit	Trajectory	Above 1000	--	66.41%
(Shi and Zhang 2021)	LSTM	Trajectory	Above 1000	2s	86.21%
(Xu et al. 2019)	HMM	Trajectory	3410	6s	94.4%
(Ali et al. 2022)	Extra trees classifier	Trajectory	Above 1000	2s	82%
(Izquierdo et al. 2017)	SVM	Trajectory	351	3s	85%

Notes: --represents No reported.

The summary of the literature in Table 1 reveals several valuable conclusions. First, vision-based LC behavior recognition methods exhibit lower classification accuracy than other methods. Second, because simulators and natural experiments are limited by the small number of experimental participants and high data homogeneity, ensuring the model's

generalizability is challenging. Third, machine learning-based models have better classification accuracy compared to statistics-based models. Fourth, the Long Short-Term Memory (LSTM) Networks are widely used for lane change intention recognition and have made great progress in improving the accuracy of the LC behavior recognition but still have excellent potential to improve classification accuracy.

The LSTM approach has two limitations: the gradient vanishing problem and the inability to perform parallel computation (Sheng et al. 2022). To overcome the above two constraints, Temporal Convolutional Networks (TCNs), first proposed by (Bai 2018), have attracted considerable interest. TCNs are designed for processing sequential data, such as time series or natural language (Guo and Yuan 2020; Li et al. 2023; Li et al. 2020). With dilated causal convolution layers, TCNs effectively capture long-term dependencies over multiple time scales in the input sequences. Following that, TCNs have achieved significant promotion in both regression and classification tasks, involving forecasting carbon prices (Li et al. 2023), predicting wind speed (Gan et al. 2021; Li et al. 2022a), and diagnosing power converter faults (Yating et al. 2021).

The dilemma encountered by traditional end-to-end models is that to predict multiple indicators, a given model may be repeatedly trained to predict different indicators with the same input parameters, leading to computational redundancy and higher costs. To address this issue, Multi-task Learning (MTL) model was proposed first by Rich Caruana (1997) and involved training a model to learn multiple related tasks simultaneously. As a promising area in machine learning, MTL aims to improve the performance of multiple related learning tasks by leveraging useful information among them (Zhang and Yang 2018). The tasks can be supervised, semi-supervised, or unsupervised and the model is designed to take advantage of shared representations across the various tasks in order to improve performance. (Deng et al. 2017) employed the MTL framework for traffic prediction, achieving up to 18% and 30% improvement in short- and long-term predictions. (Xu et al. 2020), (Zhang et al. 2021), and (Gao et al. 2018) demonstrate the effectiveness of the MTL structure in travel time prediction areas. However, the ascendancy of MTL in driving status has not been tested. To fill the gap, this paper considers the MTL framework for LC-driving status prediction.

### **3 Naturalistic driving data**

The publicly available CitySim dataset (Zheng et al. 2022) is used in this research. The CitySim dataset is a drone-based vehicle trajectory dataset extracted from 12 locations with a sampling frequency of 30 Hz, providing accurate bounding box position information for each detected vehicle. With six lanes in two directions, a sub-dataset Freeway-B collected in Asia is chosen to verify the performance of our proposed model (Ding et al. 2023). A snapshot of the freeway-B segment is shown in Fig. 1.

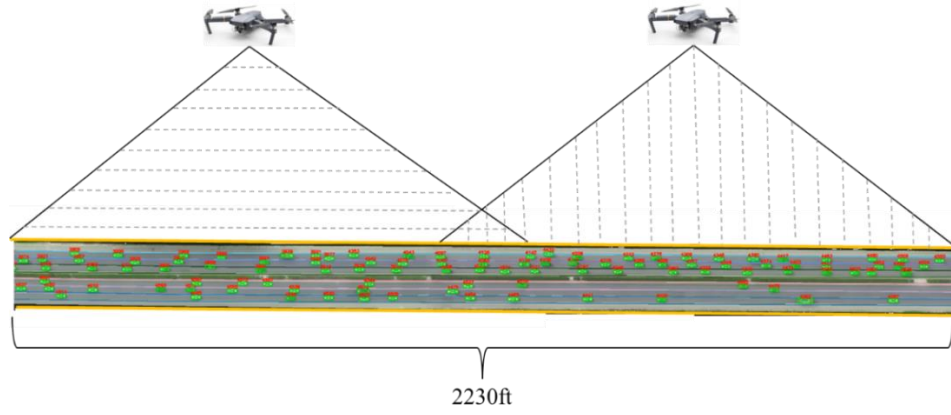


**Fig 1. A snapshot of the freeway-B segment**

The freeway-B dataset is collected simultaneously with two UAVs over a 2230-ft basic freeway segment. Totally 5623 vehicle trajectories are extracted from 60 minutes of drone videos. This study focuses on lane change processes. A total number of 1023 vehicle trajectories are extracted ultimately from the freeway-B dataset, including 545 lane-change (LC) vehicle trajectories (240 left lane change (LLC) vehicle trajectories and 305 right lane change (RLC) vehicle trajectories) and 478 lane-keeping (LK) vehicle trajectories. Lane keeping vehicle trajectories are randomly extracted.

### 3.1 Data Processing

Four significant steps are further employed for data processing with extracted vehicle trajectory data.

- 1) **Removing abnormal data.** The freeway-B dataset is collected from two stitched drone videos. The vehicle trajectory with the difference of adjacent frames greater than one is removed to avoid the effects of frame misalignment or skipping.
- 2) **Data smoothing.** Minor positioning errors might significantly affect extraction indicators (Gu et al. 2019). To reduce the negative effect of errors, a moving average (MA) method is used to smooth the trajectory, and the moving average filter is set to 0.5s. A comparison of the original trajectory and processed trajectory is shown in Fig. 2.

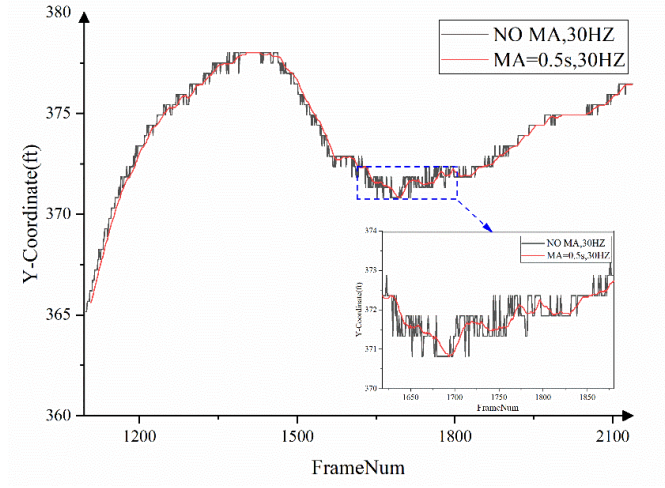


**Fig. 2** Comparison of original trajectory and processed trajectory

**3) Indicator calculation.** To accurately describe the vehicle driving status, six indicators are extracted from the two-dimensional (i.e. longitudinal and lateral) vehicle position coordinates, including the longitudinal velocity ( $v_x$ ), lateral velocity ( $v_y$ ), longitudinal acceleration ( $a_x$ ), lateral acceleration ( $a_y$ ), vehicle heading ( $\theta$ ), and vehicle heading change rate ( $\Delta\theta$ ). Furthermore, a non-linear low pass filter is employed to reduce the negative effect of measurement errors (Coifman and Li 2017). First, the vehicle speed at the  $t$ -th frame is calculated separately according to Eq. (1).

$$v_n(t) = \frac{s(t+n) - s(t-n)}{2 \cdot nT} \quad (1)$$

Where  $t$  represents the current frame,  $T$  is a constant, representing 1/30s in this research,  $n$  represents the time-step, and  $s(t-n)$  represents the vehicle's position in the frame  $t-n$ , where  $n$  takes different values, a vector  $\{v_1(t), v_2(t), \dots, v_N(t)\}$  (In this paper,  $n$  is set to 8) will be obtained. Thus, the vehicle velocity  $v(t)$  at the  $t$ -th frame is calculated by taking the median of all  $N$  time steps. The lateral velocity ( $v_y$ ) and longitudinal velocity ( $v_x$ ) can be determined based on the change in the lateral and longitudinal positions of the vehicle, respectively. With the calculated velocity, acceleration can be obtained via Eq. (2).

$$a(t) = \frac{v(t+1) - v(t-1)}{2 \cdot T} \quad (2)$$

The lateral acceleration ( $a_y$ ) and longitudinal acceleration ( $a_x$ ) also can be determined based on the change of  $v_y$  and  $v_x$ , respectively. In addition, the vehicle heading can be calculated via Eq.(3).



$$\theta_n(t) = \arctan\left(\frac{y_H(t+n) - y_R(t-n)}{x_H(t+n) - x_R(t-n)}\right) \quad (3)$$

Where  $\theta_n(t)$  represents the vehicle heading at the frame  $t$ ,  $y_H(t+n)$  is the vehicle head point longitudinal position in the frame  $t+n$ ,  $x_R(t+n)$  is the vehicle tail point horizontal position in frame  $t+n$ . It is calculated according to Eq. (4).

$$\Delta\theta(t) = \frac{\theta(t+1) - \theta(t-1)}{2T} \quad (4)$$

- 4) **Normalization.** Different metrics have different magnitudes and magnitude units, and such a situation can affect the results of data analysis. All indicators are standardized according to Eq. 5.

$$x' = \frac{x - \min(x)}{\max(x) - \min(x)} \quad (5)$$

## 4 Methodology

In this section, this paper first proposes a new modeling framework for Lane Change Intention Recognition and Status Prediction (LC-IR -SP). Then two commonly used time series processing (LSTM and TCN) models are introduced, respectively. Furthermore, a novel ensemble temporal convolutional network with Long Short-Term Memory units (TCN-LSTM) is constructed. Based MTL framework, MTL-LSTM, MTL-TCN, and MTL-TCN-LSTM models are developed. Finally, the commonly used evaluation metrics are presented.

### 4.1 Modeling framework

Fig.3 presents the framework of the proposed Lane Change Intention Recognition and Status Prediction (LC-IR -SP) model, which consists of two core modules: Lane Change Intention Recognition (LC-IR) module and Lane Change Status Prediction (LC-SP) module. The LC-IR module is a classification model used to recognize whether the vehicle produces LLC intention or RLC intention. When the LC-IR module detects that a vehicle generates a lane change intention, the LC-SP module predicts LC vehicle driving status. The LC-SP module consists of separate multi-task learning and single-task learning models for sequence-to-sequence prediction. Multi-task learning models are employed to predict related variables. As in previous studies, unrelated variables were predicted separately using a single-task model. Each module selects the highest performing sub-model by comparing the capabilities of different models. Each module retains the highest performing sub-model in the modeling framework by comparing the capabilities of different models.

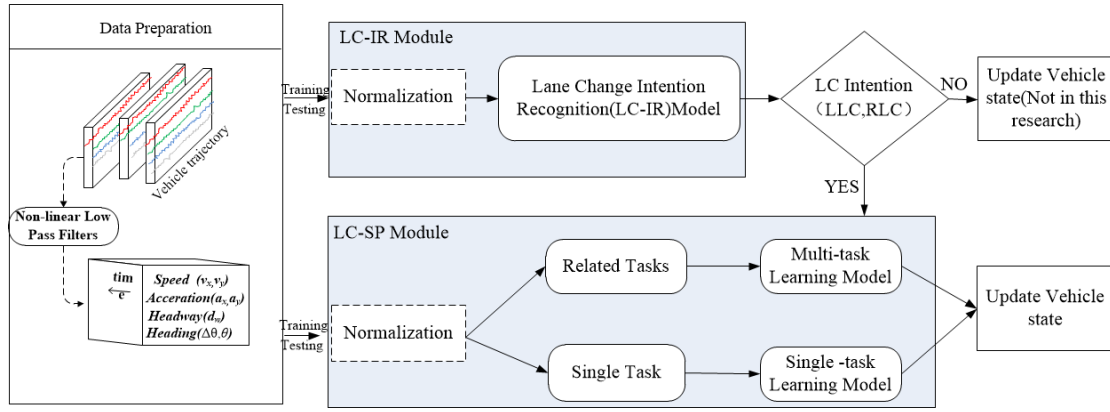


**Fig.3** Modeling framework based on deep learning

## 4.2 Input and Output

The vehicle status is influenced by other vehicles in the driving environment (Zhang et al. 2019). To fully consider the impact of various factors, the input of the combined model consists of three parts: ego vehicle (E-vehicle) information, surrounding vehicle information, and relative position information. Surrounding vehicles include the closest preceding and following vehicles in the adjacent and the current lanes. The six indicators ( $v_x, v_y, a_x, a_y, \theta, \Delta\theta$ ) were calculated for each vehicle. Limited by the video coverage, some trajectory fragments of surrounding vehicles were not recorded. A categorical variable (0 means it has recorded trajectory information; 1 means the trajectory information is missing) is added to each surrounding vehicle indicating this phenomenon. For instance, when the ego vehicle first appeared, the following vehicle (F-vehicle) is not yet in the drone videos, the following vehicle status variable is set to 1. Relative position information is the headway distance between the E-vehicle and other vehicles, as shown in Fig.4. Six indicators have been extracted to represent the relative position. If the corresponding vehicle is not recorded, the value of the variable is set to 0. A total of 54 parameters are taken as input variables.

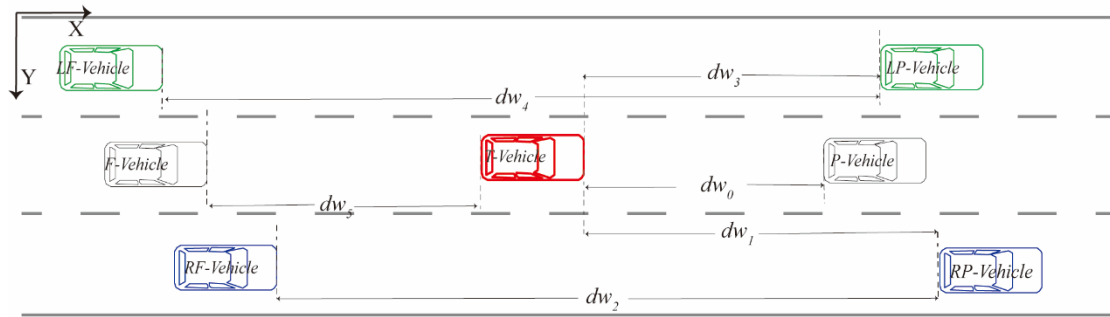


**Fig.4** the headway distance between the E-vehicle and surrounding vehicles

The integrated model produces two types of output indicators: lane change intention and future lane change vehicle driving status. As mentioned above, LC intention is divided into three categories: lane keeping (LK), left lane changing (LLC), and right lane changing (RLC). The first part of the model output is to recognize if the vehicle will make a lane change. The second part of the output is to predict the status of the lane change vehicles, represented by

those six parameters( $v_x, v_y, a_x, a_y, \theta, \Delta\theta$ ). Velocity ( $v_x, v_y$ ) and heading ( $\theta$ ) can be regarded as macroscopic indicators that reflect the aggregated effects of prior driving behavior.

Meanwhile, acceleration ( $a_x, a_y$ ) and rate of change of heading angle( $\Delta\theta$ ), used as microscopic indicators, indicate the driving behavior that the driver is about to perform, reflecting changes in the throttle, brake pedal, and steering angle of the vehicle respectively. The input and output indicators are presented in Table 2.

**Table 2** Inputs and outputs of the integrated model

Type	Variable	Variable descriptions
Inputs	$E-, P-, F-, LP-, LF-, RP-, RF-v_x$	The longitudinal velocity of E-vehicle and surrounding vehicle (ft/s)
	$E-, P-, F-, LP-, LF-, RP-, RF-v_y$	The lateral velocity of E-vehicle and surrounding vehicle (ft/s)
	$E-, P-, F-, LP-, LF-, RP-, RF-a_x$	The longitudinal acceleration of E-vehicle and surrounding vehicle (ft/s <sup>2</sup> )
	$E-, P-, F-, LP-, LF-, RP-, RF-a_y$	The lateral acceleration of E-vehicle and surrounding vehicle (ft/s <sup>2</sup> )
	$E-, P-, F-, LP-, LF-, RP-, RF-\theta$	The heading of E-vehicle and surrounding vehicle (degree)
	$E-, P-, F-, LP-, LF-, RP-, RF-\Delta\theta$	The heading change rate of E-vehicle and surrounding vehicle (degree/s)
	$dw_0, dw_1, dw_2, dw_3, dw_4, dw_5$	Space headway between E-vehicle and surrounding vehicle (ft)
	$P-, F-, LP-, LF-, RP-, RF-val$	0 means it has recorded trajectory information; 1 means the trajectory information is missing
Output 1	Lane-change intention	Lane keeping (LC), left lane changing (LLC), or right lane changing (RLC)
Output 2	$v_x, v_y, a_x, a_y, \theta, \Delta\theta$	The status of E-vehicle in the future

**Note:** “T-” represents the ego vehicle; “P-” represents the closest preceding vehicle in the same lane; “F-” represents the closest following vehicle in the same lane; “LP-” represents the closest preceding vehicle in the adjacent left lane; “LF-” represents the closest following vehicle in the adjacent left lane; “RP-” represents the closest preceding vehicle in the adjacent right lane; “RF-” represents the closest following vehicle in the adjacent right lane;

### 4.3 Temporal convolutional networks

TCN consists of causal convolution and dilated convolution (Bai, 2018; Guo and Yuan 2020). Causal convolutions are used to ensure the temporal dependencies of the input data. Given an input sequence  $x_0, x_1, \dots, x_n$  and the corresponding output sequence  $y_0, y_1, \dots, y_n$ , the causality constraint causal convolutions ensure that the output  $y_t$  at time  $t$  is only determined by the input sequence  $x_0, x_1, \dots, x_t$ . The one-dimensional fully-convolutional network (1DFCN) architecture is employed to produce the same length output as the input (Long et al. 2015). The TCNs can be expressed as Eq. (6).

$$TCNs = 1D\ FCN + causal\ convolutions \quad (6)$$

Using causal convolution, it is theoretically possible to generate TCNs. However, the receptive field of causal convolution is constrained, making it difficult to capture the

correlation between points in a long-term temporal sequence. For instance, if the output is related to the previous 100 elements, the deep causal convolution should be 99. The extremely deep complexity network or large filters can make training difficult and lead to model degradation (He et al. 2016). Hence, dilated convolutions were added to causal convolutions, enabling an exponentially large receptive field. For a filter  $f: \{1, 2, \dots, k-1\}$ , the dilated convolution operation  $F$  on the element  $s$  of a 1-D sequence  $x \in R^n$  is formulated as Eq. (7) (Bai, 2018).

$$F(s) = (x *_{d} f)(s) = \sum_{i=0}^{k-1} f(k) \cdot x_{s-d \cdot i} \quad (7)$$

Where  $d$  is the dilation parameter and is used to control the size of the interval,  $k$  is the filter size and represents the number of convolution kernels,  $*$  is the convolution operator,  $s - d \cdot i$  accounts for the direction of the past. A dilated convolution will backward to a full convolution when  $d = 1$ . The dilated causal convolution structure is depicted in Fig. 5.

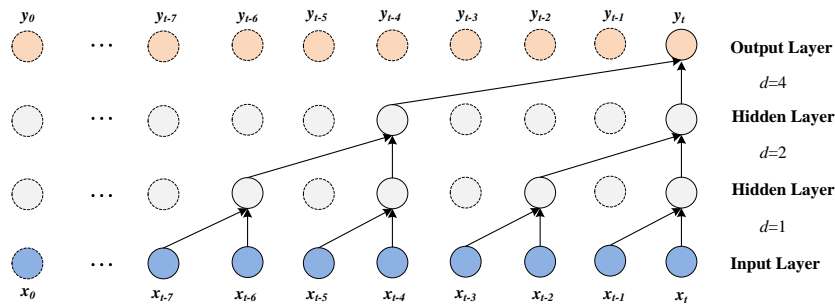


**Fig.5** A dilated causal convolution with dilation factors  $d = 1, 2, 4$  and kernel size  $k = 2$  (van den Oord et al. 2016)

As shown in Fig. 5, the kernel size is set to 2, and the depth of the causal convolution is 3. The convolution indicated that the output at time  $t$  is associated with the input points from time  $t-7$  to time  $t$ . Residual blocks are used to address disappearance and gradient expansion in TCNs. Utilizing techniques such as longer convolutional kernels and residual connections allows TCN to capture long-term dependencies. As shown in Fig. 6, the rectified linear unit (ReLU) is utilized as an activation function, and batch normalization is used as the convolutional filter. A  $1 \times 1$  convolution is added in the residual block when the input and output data have different lengths.

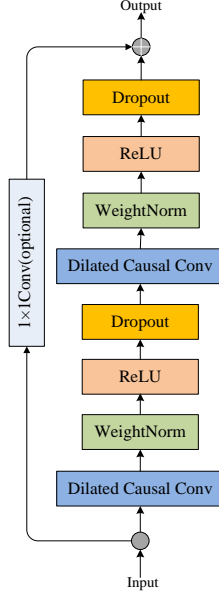


**Fig.6** TCN residual block (Bai, 2018)

By adjusting dilation parameters, the amount of information received by the TCN can be changed. The receptive field of the TCN can be calculated as Eq.(8):

$$R_{field} = 1 + (K - 1) \times N_{stack} \times \sum_i d_i \quad (8)$$

Where  $R_{field}$  represents the receptive field of the TCN,  $K$  is the filter size,  $N_{stack}$  represents the number of stacks,  $d_i$  represents the dilation parameter the in  $i$ th layer.

## 5.2 Long Short-Term Memory (LSTM) Network

LSTM is a commonly used recurrent neural network (RNN)(Gao et al. 2020; Wang et al.2022; Shi and Zhang 2021). LSTM adopts a gating mechanism that selectively retains or forgets information, effectively enhancing the long-term dependency modeling capability of traditional RNNs. A typical LSTM block is configured mainly by an input gate  $i_t$ , forget gate  $f_t$ , and output gate  $o_t$ . These gates are computed as follows.

$$i_t = \sigma(W_i x_t + U_i h_{t-1} + b_i) \quad (9)$$

$$f_t = \sigma(W_f x_t + U_f h_{t-1} + b_f) \quad (10)$$

$$o_t = s(W_o x_t + U_o h_{t-1} + b_o) \quad (11)$$

Where  $\sigma$  represents the sigmoid activation function;  $x_t$  represents the input sequence at time  $t$ ;  $h_{t-1}$  represents the hidden state;  $W$  is the parameter matrix at time  $t$  and represents the input weight;  $U$  is the parameter matrix at time  $t - 1$ , and represents the recurrent weight;  $b_i$ ,  $b_f$ , and  $b_o$  represents bias. The internal update state of the LSTM recurrent cells can be expressed as:

$$c_t = f_t \odot c_{t-1} + i_t \odot \tilde{c}_t \quad (12)$$

$$h_t = o_t \odot \tanh(c_t) \quad (13)$$

Where  $\odot$  represents vector element-wise product,  $c_t$  is the memory cell at time  $t$ ,  $\tilde{c}_t$  is the candidate memory at time  $t$ ,  $h_t$  is the outcome at time  $t$ . A detailed LSTM block structure is shown in Fig.7.

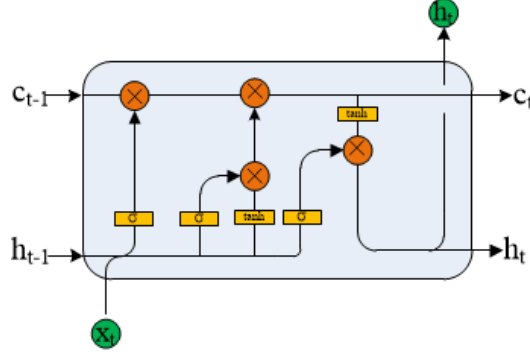
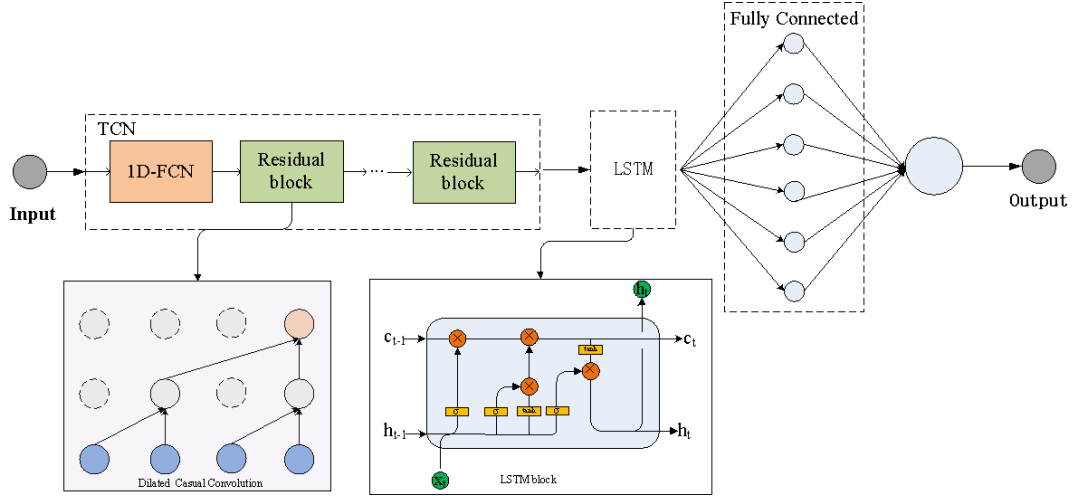


Fig.7 LSTM block structure

### 5.3 TCN-LSTM Network

Both LSTM and TCN networks are commonly used to process sequential data (Ren et al. 2023; Song et al. 2022). By using a dilated convolutional architecture, TCN can perform parallel computations across time steps, whereas LSTM requires sequential processing. Thus, TCN is not susceptible to gradient vanishing and explosion issues, unlike LSTM, and can effectively capture long-term dependencies, making it better suited for processing large sequences. On the other hand, LSTM is capable of capturing long-term dependencies and can effectively handle tasks that require long-term memory by utilizing internal memory units that selectively remember or forget information from previous time steps. Based on the structure of the TCN and LSTM model, a novel ensemble temporal convolutional network with Long Short-Term Memory units (TCN-LSTM) is developed in this research. Fig.8 presents the structure of the TCN-LSTM network. The multi-dimensional time sequences are taken as input variables. Then, the TCN layer is performed to extract temporal features from the input time series, the LSTM layer filters information through three gates further, and finally, the fully connected layer is applied to output results. The TCN-LSTM model combines the efficient temporal modeling of the TCN with the memory retention of the LSTM, making it robust to noise and scalable for large datasets.



**Fig. 8** TCN-LSTM Network Structure

#### 5.4 Multi-task learning framework

MTL can be viewed as a generalization of multi-label learning and multi-output regression (Zhang and Yang 2018) and has the advantages of improving data efficiency, generalization ability, regularization ability, and overall performance (Deng et al, 2017; Zhang et al, 2021). It is designed to leverage a shared representation at the bottom layer and simultaneously enables learning multiple related tasks. For the  $k$ th task, the output  $y_k$  in MTL can be expressed as:

$$y_k = h^k \left( f(x) \right) \quad (14)$$

Where the  $f$  function represents the shared-bottom network,  $h^k$  denotes the  $k$ th tower network, and  $x$  is the input variable vector. Compared to single-task learning, multi-task learning framework can share information among different tasks, reduce training time, and improve the efficiency of data utilization (Standley et al. 2020). Given 3 learning tasks, the comparison of single-task and multi-task learning architecture based on single-layer networks is shown in Fig.9. Task 1, Task 2, and Task 3 are three related output variables that share common input indicators. Using a single-task learning model requires building three separate models, but in the multi-task learning framework, only one model is required to be constructed with three outputs.

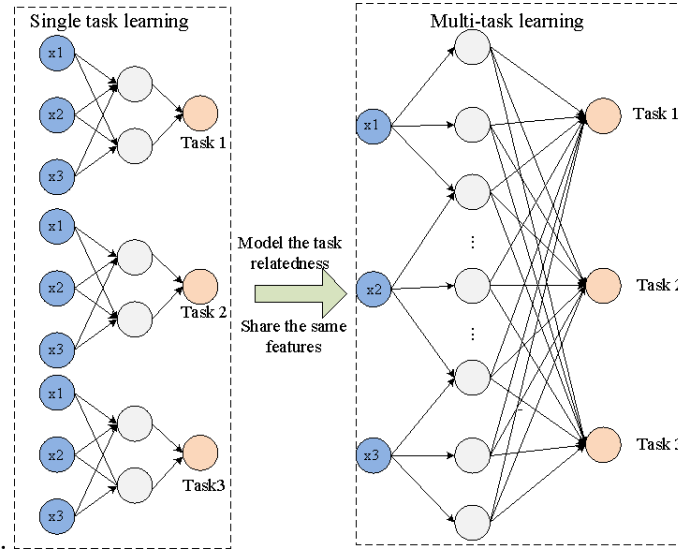


**Fig.9** The comparison of single-task and multi-task learning architecture

The loss function is a critical component of multi-task learning. How design the loss function for multi-task learning is crucial to determining the performance of the model. A common approach is to use a linear function to directly combine these loss functions, as in Equation (15).

$$Loss_{total} = \sum_i \omega_i Loss_i \quad (15)$$

Where  $Loss_{total}$  represents the cumulative loss of all tasks,  $Loss_i$  is the loss of the  $i$ -th task, and  $\omega_i$  is the weight of the  $i$ -th task. By adjusting  $\omega_i$ , the model performance for the  $i$ -th task can be changed. For instance, if there is a main task in all the tasks, increasing the loss weight of the main task can improve the model performance for it. In this study, all tasks are considered equally important with assigned equal weights.

Based on the multi-task model framework, three multi-task models (MTL-LSTM, MTL-TCN, MTL-LSTM-TCN) are first developed in this study. The model structures are shown in Fig.10. In the proposed MTL model, the LSTM and TCN layers are utilized to extract temporal features in three models, respectively. Then, fully connected layers are employed to output prediction results for each variable.



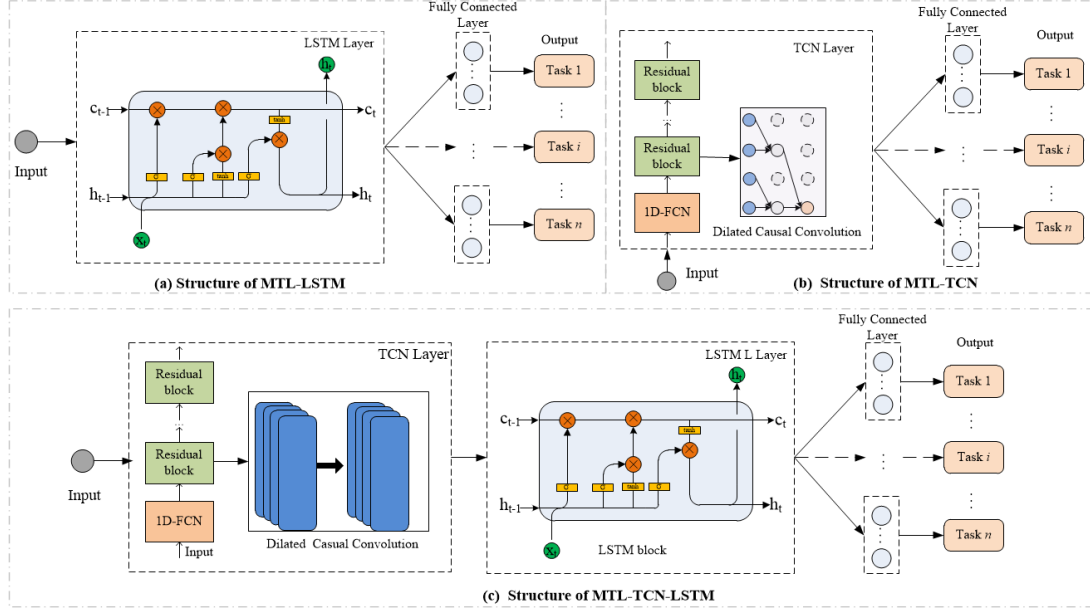


**Fig. 10** The structure of the proposed MTL models

## 5.6 Evaluation indexes

The modeling framework proposed includes classification models and sequence prediction models. The performance of classification models is evaluated from two aspects. One is the overall performance of the classification, and the other is the recognition performance of each class (Yang et al. 2021). The two indexes, precision and recall, are used to evaluate the detection performance of each class. The accuracy index measures the overall performance of the model. The three indexes can be calculated as follow,

$$Accuracy = \frac{T}{T + F} \quad (16)$$

$$Precision = \frac{TP}{TP + FP} \quad (17)$$

$$Recall = \frac{TP}{TP + FN} \quad (18)$$

Where T represents the number of correctly classified samples, F represents the number of incorrectly classified samples, TP is the number of correctly classified samples in a given class, FP is the number of incorrectly classified samples in a given class, FN denotes the number of incorrectly classified samples in a given class. The two indexes, Mean Absolute Error (MAE) and Root Mean Square Error (RMSE) are employed to evaluate the performance of sequence prediction models. The definitions are as follows,

$$MAE = \frac{1}{N} \sum_{i=1}^N |y_i - \hat{y}_i| \quad (19)$$

$$RMSE = \sqrt{\frac{1}{N} \sum_{i=1}^N (y_i - \hat{y}_i)^2} \quad (20)$$

Where  $y_i$  is the observed value of the  $i$ -th output,  $N$  is the number of outputs,  $\hat{y}_i$  represents the predicted value of  $y_i$ . The prediction model with lower MSE and RMSE values performs better.

## 6 Results and discussion

To testify the feasibility of our modeling framework and compare the performance of the proposed models, the lane change intention recognition (LC-IR) model and the lane change status prediction (LC-SP) model are developed in this section, respectively. And we selected 545 LC vehicle trajectories and 478 LK vehicle trajectories for training and testing the lane change intention recognition model. However, only LC vehicle trajectories were used to train and test the lane change status prediction model.

### 6.1 Parameter setting

The parameter setting will affect the performance of the model. To obtain optimal parameter settings in two modules, some sensitivity experiments were conducted to test LSTM, TCN, and TCN-LSTM recognition and predictive performance separately. The final parameter settings could be found in Table 3.

**Table 3** Parameter setting in LC-IR-SP model.

Module	Model	Parameter	Description	Value
	General Settings	Activate function	The function to fully connected layer	Relu function
		Dropout	The rate used in the dropout layer	0.3
		Batch size	Number of samples passing through to the network at one time	128
		Training epochs	Number of a training update	20
		Dilation factors (TCN)	The size of dilated convolution interval. Depends on the input time series length.	$\{2^1, 2^2, 2^3, \dots, 2^n\}$
		kernel_size (TCN)	The number of units from the previous layer	2
		nb_filters (TCN)	The number of filters	64
		Units (LSTM)	Number of neurons in the hidden layer	64
LC-IR	General Settings	Loss function	The function to calculate loss	Categorical_crossentropy
		Output layer activation function	The function to activate output	Softmax
		Optimizer	The function to minimize loss	rmsprop
	LSTM	depth (LSTM)	Number of LSTM layer	2
LC-SP	General Settings	Loss function	The function to calculate loss	mean_squared_error
		activation function	The function to activate output	Tanh function
		Optimizer	The function to minimize loss	adam
	LSTM	depth (LSTM)	Number of LSTM layer	2

## 6.2 Lane Change Intention Recognition

The vehicle's lane change intentions are defined as some LC operational behavior produced before the lane change. They are generally classified into three situations: lane keeping (LK) intention, left lane changing (LLC) intention, and right lane changing (RLC) intention. To select an appropriate algorithm for classifying lane change intentions, this section compares the performance of three algorithms: LSTM, TCN, and TCN-LSTM

### 6.2.1 Lane-change intention labeling

In this study, the start time of the LC process is determined as the moment when the front boundary point of vehicles touches the lane boundary (Zhang et al. 2023). The annotation procedure determines the LC intention start time as 3 seconds forward the start time of LC processes. The start point of LC processes is considered to be the end point of LC intention. A total of 24,092 frames are labeled as RLC points, while 19,792 frames are labeled as LLC points. Fig. 11 shows the detailed labeling processes. If the extracted sequence endpoint is located between the start time of the LC process and the LC intention start time (at least one RLC point or LLC point is included in the sequence), it is labeled as either Left Lane Change (LLC) or Right Lane Change (RLC); Otherwise, it is labeled as Lane Keeping(LK).

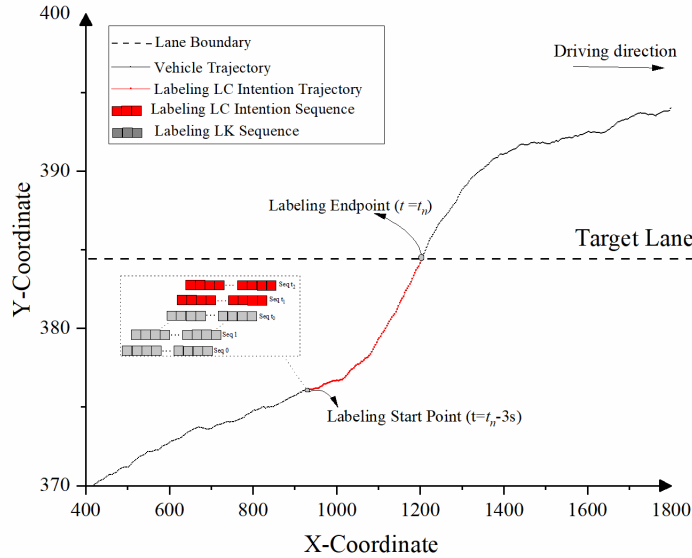
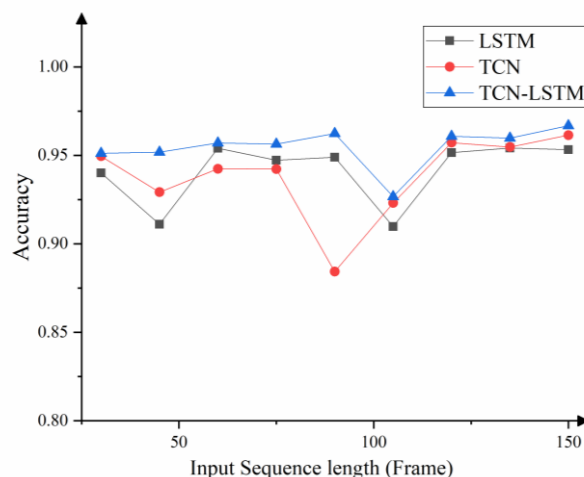


Fig.11 Lane-change intention labeling process

### 6.2.2 Results of LC intention recognition models

To investigate the effect of input sequence length on classification outcomes, the performance of LSTM, TCN, and TCN-LSTM models with varying input durations is evaluated. With an interval of 15 frames, a total of 10 input lengths are extracted from 30 frames(1s) to 150 frames(5s). The dataset is randomly split into a training set and a test set

with a ratio of 8:2. For training the LC intention classification model, 80% of total data is applied, and 20% data is used for testing the classification performance. The accuracy index is applied to measure the performance of three models.



**Fig.12** Accuracy comparison of LSTM, TCN, and TCN-LSTM

Fig.12 illustrates the comparison of overall accuracy among the three models. From the figure, we can observe that each model has good classification performance (above 85%), even though the three models are slightly different among different durations. The results reveal that lane-change intention extracted from vehicle trajectories is reasonable, which can distinguish characteristics of LK, RLC, and LLC. For input data with the same time scale, the proposed TCN-LSTM model outperforms the other models in terms of classification accuracy. With 150 frames as the input length, the best classification accuracy was achieved for all three models. Hence, a time duration  $T = 150$  frame(5s) is chosen as input sequence lengths. Finally, 22160 RLC sequences and 15410 LLC sequences are extracted. To maintain data balance, 18000 LK sequences are randomly extracted from the raw dataset. Confusion matrices for three models: LSTM, TCN, and TCN-LSTM are shown in Fig. 13.

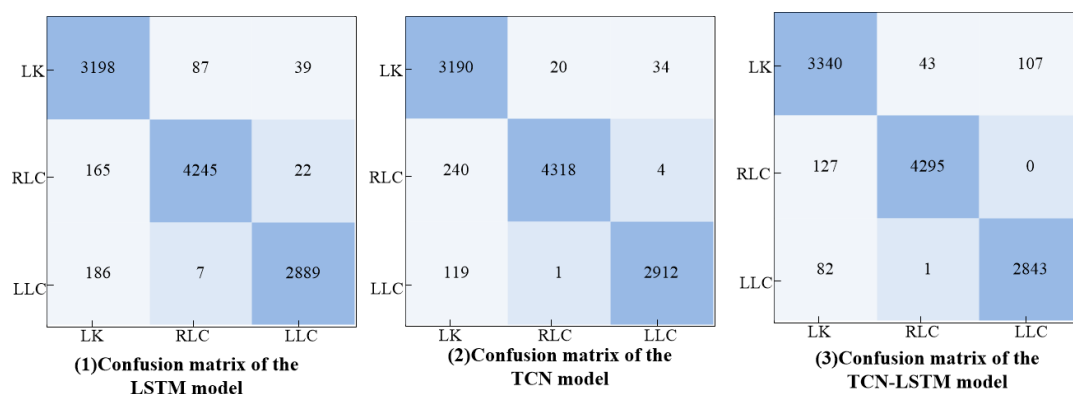


**Fig.13** Confusion matrix of classification models

The precision and recall indexes were evaluated through the confusion matrixes. With an input length of 150 frames, the comparison results are displayed in Table 4. It could be seen from the table that the overall classification performance using the TCN-LSTM model is 96.67%, improved by 0.27% and 1.34% compared to using the TCN and LSTM model, respectively. The precision of the TCN-LSTM model for the LK class is 94.19%, while the TCN and LSTM models exhibit precisions of 89.88% and 90.10%, respectively. This indicates that the proposed TCN-LSTM model has higher accuracy for the LK class samples compared to the TCN and LSTM models, with improvements of 4.31% and 4.09%, respectively. The variation in recognition precisions among the three models for the RLC and LLR classes is minor, remaining within a 1.5% range. And the TCN-LSTM model exhibits high recall rates with 97.13% and 97.16% for the RLC and LLR classes, respectively. Nonetheless, when considered individually, the maximum deviation in classification accuracy for each model is 4.8% for TCN-LSTM, 10.09% for TCN, and 7.73% for LSTM. The maximum difference in recall index for each model is 1.46% for TCN-LSTM, 3.6% for TCN, and 2.48% for LSTM. The result indicates that the proposed TCN-LSTM model provides more balanced results. In summary, the proposed TCN-LSTM model provides a promising solution for driving intention classification tasks, as it outperforms other models in terms of classification accuracy.

**Table 4** Evaluation results of TCN-LSTM model (input length is 150 frames)

Model	Directions	Precision	Recall	Accuracy
TCN-LSTM	Lane-keeping	94.19%	95.70%	96.67%
	Right lane change	98.99%	97.13%	
	Left lane change	96.37%	97.16%	
TCN	Lane-keeping	89.88%	98.33%	96.14%
	Right lane change	99.97%	94.73%	
	Left lane change	98.71%	96.04%	
LSTM	Lane-keeping	90.10%	96.21%	95.33%
	Right lane change	97.83%	95.78%	
	Left lane change	97.79%	93.73%	

### 6.3 Lane Change Status Prediction

As mentioned in Section 4.2, vehicle status involves six indicators:  $v_x, v_y, a_x, a_y, \theta, \Delta\theta$ . Similarly, predicting lane change status requires the simultaneous prediction of these six indicators. In this section, the Pearson coefficient is used to investigate the relationship between those output indicators. Then three proposed multi-tasking learning models are used to capture the intrinsic relationship among these related indicators.

#### 6.3.1 Correlation Analysis

Multi-task learning (MTL) involves jointly learning multiple output indicators. The underlying assumption behind this approach is that all output indicators are related. Typically, the relationship between tasks could significantly affect the predictive quality of multi-task models (Ma et al. 2018). Hence, the Pearson coefficient is employed to investigate whether there is an association between the variables, formulated as.

$$r = \frac{\sum_{i=1}^n (x_i - \bar{x})(y_i - \bar{y})}{\sqrt{\sum_{i=1}^n (x_i - \bar{x})^2} \sqrt{\sum_{i=1}^n (y_i - \bar{y})^2}} \quad (21)$$

Where  $x_i$  represents the  $i$ th value of the indicator  $x$ ,  $\bar{x}$  and  $\bar{y}$  represent the average value of indicator  $x$  and  $y$ ,  $r$  represents the Pearson coefficient and takes values in the range  $[-1,1]$ . The larger the absolute value of  $r$ , the stronger the correlation. In this research, only the indicators with an absolute value of Pearson coefficient greater than 0.2 are considered to be related (Qin et al. 2023; Ran 2021). There are two types of vehicle information are used to calculate the Pearson coefficient separately: lane-keeping (LK) vehicles and lane-changing (LC) vehicles. The LC vehicle information used is the driving intention labeled segment defined in Fig.11. To mitigate the effect of sample imbalance on the results, 200 samples from each LK vehicle trajectory are extracted randomly. The Pearson coefficient heat map is shown in Fig.14.

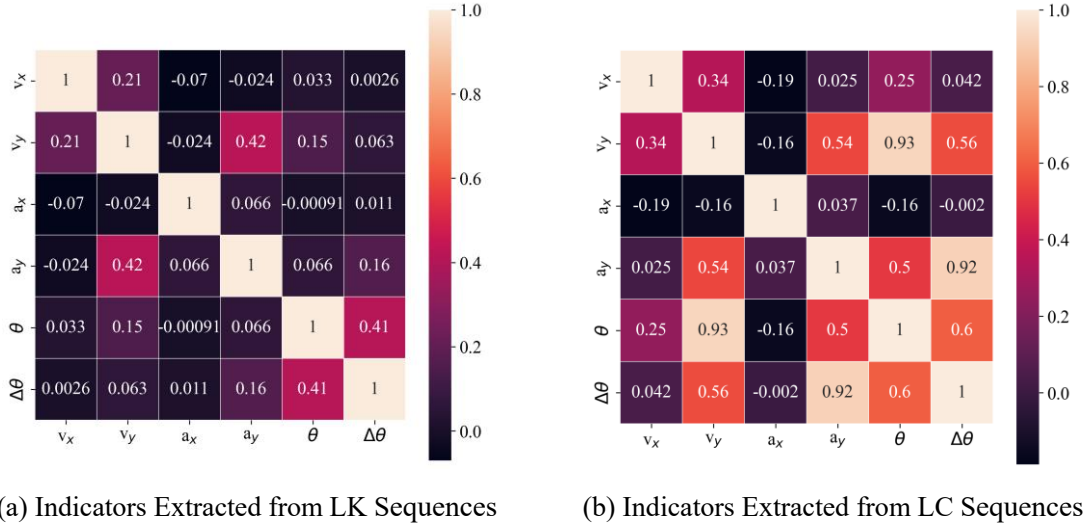


**Fig.14** Pearson coefficient heat map

Fig.14 illustrates the Pearson coefficient between  $v_x$  and  $v_y$ ,  $a_y$  and  $v_y$ ,  $\theta$  and  $\Delta\theta$ , which are greater than 0.2 in both types of sequences. The indicators extracted from the LK sequences exhibit a stronger correlation than those extracted from LC sequences. No significant correlation was found between lateral acceleration ( $a_y$ ) and other indicators. Furthermore, the main discrepancies are observed between the heading-related indicators ( $\theta$  and  $\Delta\theta$ ) and the

velocity-related indicators ( $v_x$ ,  $v_y$ , and  $a_y$ ). For lane-changing processes, strong correlations were observed between  $v_x$  and  $\theta$  (0.25),  $v_y$  and  $\Delta\theta$  (0.56),  $a_y$  and  $\theta$  (0.92), and  $v_y$  and  $\theta$  (0.93), indicating a close relationship between these variables. In contrast, no significant relationship was found in lane-keeping processes between heading-related indicators ( $\theta$  and  $\Delta\theta$ ) and velocity-related indicators ( $v_x$ ,  $v_y$ , and  $a_y$ ). The result could be explained by the fact that during a lane change, drivers have to adjust their driving direction and velocity to achieve the desired purpose. However, during the lane-keeping phase without a specific task, the changes in heading and speed are random and separate from each other.

### 6.3.2 Results of LC status prediction models

With a focus on the purpose of the study, only sequences labeled as RLC and LLC are utilized in this section. Eighty percent of the extracted samples are used to train the model, while the remaining 20% are used for validating the performance. With 1s interval (indicators take an average of 60 frames), lane-change vehicle status in the next 2s are predicted. The input sequence length is set to 150 frame(5s). As mentioned above, LC vehicle status prediction involves six output variables ( $v_x$ ,  $v_y$ ,  $a_x$ ,  $a_y$ ,  $\theta$ ,  $\Delta\theta$ ), in which  $v_x$ ,  $v_y$ ,  $a_x$ ,  $\theta$ , and  $\Delta\theta$  are related output variables, and  $a_y$  is not correlated with other variables. Actually, without considering the correlation among output variables, three models, including LSTM, TCN, and TCN-LSTM, could be employed individually to address such sequence-to-sequence prediction issues. However, the expected six output variables ( $v_x, v_y, a_x, a_y, \theta, \Delta\theta$ ) are simultaneously influenced by the surrounding environment. To improve prediction accuracy, three multi-task model (MLT-LSTM, MLT-TCN, MLT-LSTM-TCN) are trained with the same input and output variables.

A total of 18 single-task learning models were trained using LSTM, TCN, and TCN-LSTM for six metrics ( $v_x, v_y, a_x, a_y, \theta, \Delta\theta$ ), respectively. Considering the intrinsic relationship among outcome factors, MTL-LSTM, MTL-TCN, and MTL-LSTM-TCN were trained for five related variables ( $v_x, v_y, a_y, \theta, \Delta\theta$ ). The prediction results are listed in Table 5. For the output variable  $a_x$ , the TCN model has the lowest MAE and RMSE values compared to the other models. Specifically, the RMSE value of TCN is 1.4023 ft/s<sup>2</sup>, which is only 88.04% and 84.33% of the values of TCN-LSTM and LSTM, respectively. The results reveal that the TCN model has a superior predictive performance for the longitudinal acceleration  $a_x$ .

**Table 5** Model result comparison

Model	Metrics	Task					
		$v_x$	$v_y$	$a_x$	$a_y$	$\Delta\theta$	$\theta$
TCN-LSTM	MAE	2.96752	0.6192	1.2025	0.716	1.5339	1.6105
	RMSE	4.1352	0.8357	1.5927	0.9724	1.73032	1.8161
TCN	MAE	2.9772	0.596	1.0640	0.6693	8.1598	1.89449

	RMSE	4.13462	0.79356	1.4023	0.9224	10.604	2.4087
LSTM	MAE	2.81709	0.5722	1.2565	0.6929	2.37573	1.42012
	RMSE	3.92602	0.7044	1.6628	0.9375	3.04963	1.84598
MTL-TCN-LSTM	MAE	2.3362	0.61037	--	0.68375	1.1794	0.65262
	RMSE	2.8383	0.824071	--	0.951337	1.5759	0.85905
MTL-TCN	MAE	1.9828	0.5474	--	0.6485	2.94508	1.5665
	RMSE	2.5341	0.7516	--	0.916	3.8759	2.0624
MTL-LSTM	MAE	1.5718	0.518	--	0.6192	1.8532	0.8271
	RMSE	2.0093	0.6949	--	0.8489	2.3483	1.0853

The table also presents the performances of three MTL models. The MTL-LSTM model has a good overall predictive performance for  $v_x$ ,  $v_y$ , and  $a_y$ . However, for  $\Delta\theta$  and  $\theta$ , the MTL-TCN-LSTM has higher prediction accuracy and better performance. In addition, the prediction performances of the proposed three MTL models were compared with the corresponding single-task models (TCN, TCN-LSTM, and LSTM). The improvement ratio is calculated based on Eq.(22).

$$p_i = 1 - \frac{m_i}{s_i} \quad (22)$$

Where  $m_i$  represents the evaluation index (RMSE, MAE) value of  $i$ -th task using multi-task model,  $s_i$  represents the evaluation index (RMSE, MAE) value of  $i$ -th task using the corresponding single-task models,  $p_i$  is evaluation index improvement ration of task  $i$  using MTL model comparing to single-task model. A positive value of  $p_i$  indicates that the multi-task model outperforms the corresponding single-task models in predicting task  $i$ , while a negative value indicates the opposite. Table 6 presents the result of the improvement in prediction performance.

As is evident in Table 6, multi-tasking learning model over five indicators provide markedly increased performance compared to the corresponding single-task model. From an overall perspective, the multi-tasking learning models provide an average reduction of 24.24% and 22.86% in the Mean Absolute Error (MAE) and Root Mean Square Error (RMSE), respectively. From the perspective of the model, MTL-TCN-LSTM network outperforms TCN-LSTM model, with an average improvement of 21.96% in MAE and 19.31% in RSME. MTL-TCN model has an average improvement rate of 25.18% in MAE and 24.50% in RMSE. Similarly, MTL-LSTM significantly improved MAE by 25.61% and RSME by 24.77%. From the perspective of indicators, the three multi-task models proposed exhibit an average improvement of 36.26% in MAE and 35.84% in RSME for three indicators:  $v_x$ ,  $\Delta\theta$ , and  $\theta$ . Additionally, there is an average improvement of 6.25% in MAE and 3.38% in RSME for indicators  $a_y$ , and  $v_y$ . The performance improvement resulting from considering the relationship between output variables may be critical to accurately predicting driving status.



**Table 6** Performance improvement rate of prediction

Model	Index	$v_x$	$v_y$	$a_y$	$\Delta\theta$	$\theta$	Mean value
MTL-TCN-LSTM vs TCN-LSTM	MAE	21.27%	1.43%	4.50%	23.11%	59.48%	21.96%
	RSME	31.36%	1.39%	2.17%	8.92%	52.70%	19.31%
MTL-TCN vs TCN	MAE	33.40%	8.15%	3.11%	63.91%	17.31%	25.18%
	RSME	38.71%	5.29%	0.69%	63.45%	14.38%	24.50%
MTL-LSTM vs LSTM	MAE	44.20%	9.47%	10.64%	21.99%	41.76%	25.61%
	RSME	48.82%	1.35%	9.45%	23.00%	41.21%	24.77%
Mean value	MAE	32.95%	6.35%	6.08%	36.33%	39.51%	24.24%
	RSME	39.63%	2.67%	4.10%	31.79%	36.09%	22.86%

## 7 Conclusions and future work

Lane change behavior is a basic driving behavior that largely impacts traffic efficiency and safety. This paper uses vehicle trajectory data to develop a lane change intention recognition (LC-IR) model and a lane change status prediction (LC-SP) model. To improve classification and prediction performance, a novel ensemble temporal convolutional network with Long Short-Term Memory units and three multi-task models (MLT-LSTM, MLT-TCN, MLT-LSTM-TCN) are developed. Furthermore, a unified modeling framework for lane-change intention recognition and lane-change status prediction (LC-IR-SP) is proposed. To validate the reliability of the proposed modeling framework, a total number of 1023 vehicle trajectories was first extracted from the CitySim dataset. Then, data processing, indicator calculation, normalization, were conducted. The Pearson coefficient was used to investigate the relationship between the output variables.

The classification performance of LSTM, TCN, and TCN-LSTM models with varying input durations is compared in LC-IR module. From the results, it is evident that the proposed TCN-LSTM model outperforms other models for driving intention recognition at any input time series length. With 150 frames as the input length, the best classification accuracy was achieved for all three models. Specifically, the overall classification performance using the TCN-LSTM model is 96.67%, improved by 0.27% and 1.34% compared to using the TCN and LSTM model. The precision and recall scores of over 94% for three classifications indicate that the TCN-LSTM model is highly effective in driving intention recognition. Hence, the proposed TCN-LSTM model provides a promising solution for driving intention classification tasks, as it outperforms other models in terms of classification accuracy and provides more balanced results. It can be chosen in LC-IR module to classify driving intentions using 150 frames long input time series.

For LC driving status prediction, this research developed three multi-task models: MLT-LSTM, MLT-TCN, and MLT-LSTM-TCN. The results showed that the proposed MTL-model outperforms the corresponding single-task learning models. Moreover, the MTL-LSTM network had a better predictive performance for  $v_x$ ,  $v_y$ , and  $a_y$ , while the MTL-TCN-LSTM

model had higher prediction accuracy for  $\Delta\theta$  and  $\theta$ . Hence, to obtain good prediction results, both MTL-LSTM and MTL-TCN-LSTM models are selected in the LC-SP module. Only the predictive result of  $v_x$ ,  $v_y$ , and  $a_y$  in MTL-LSTM model, and the predictive result of  $\Delta\theta$  and  $\theta$  in MTL-TCN-LSTM model are used. The comparison of the three single-output prediction models (LSTM, TCN, LSTM-TCN) showed that the TCN model has the lowest MAE and RMSE values for indicator  $a_x$ . Therefore, the TCN model was selected to predict indicator  $a_x$ .

The research show that the proposed TCN-LSTM outperforms both LSTM and TCN models in lane change intention recognition. Considering the correlation of related indicators could improve the prediction accuracy of the model. This proposed model framework is conducted based on vehicle trajectory data, which can identify vehicle lane changing behavior, and also can predict the lane-change vehicle statutes. According to the obtained index  $v_x$ ,  $v_y$ ,  $a_y$ ,  $a_x$ ,  $\theta$ , and  $\Delta\theta$ , the real-time traffic conflict index can be calculated (Chen et al. 2020a). According to the index  $a_y$ ,  $a_x$ ,  $\theta$ , and  $\Delta\theta$ , it can be determined whether the driver has taken the avoidance behavior. This study also has some study limitations. In the multi-task learning model, we use the same weights for the loss function of each task. To eliminate the effect of magnitude on the prediction results, all input and output vectors are normalized. In the future, the prediction accuracy can be further improved by using the adaptive loss function. For instance, if there is a main task in all the tasks, increasing the loss weight of the main task could improve the model performance.

## Acknowledgments

This research is funded by the National Natural Science Foundation of China (No. 71871059), Postgraduate Research & Practice innovation Program of Jiangsu Province (No.KYCX22\_0270), and China Scholarship Council (CSC)

## Reference:

- Ali, Hussain, Bliemer, Zheng, and Haque. 2022. 'Predicting and explaining lane-changing behaviour using machine learning: A comparative study', *Transportation Research Part C: Emerging Technologies*, 145.
- Bagloee, Tavana, Asadi, and Oliver. 2016. 'Autonomous vehicles: challenges, opportunities, and future implications for transportation policies', *Journal of Modern Transportation*, 24: 284-303.
- Bai. 2018. 'An empirical evaluation of generic convolutional and recurrent networks for sequence modeling', *arXiv*.
- Cabri, Gherardini, Montangero, and Muzzini. 2021. 'About auction strategies for intersection management when human-driven and autonomous vehicles coexist', *Multimedia Tools and Applications*, 80: 15921-36.
- Cao, Li, and Chan. 2020. "A CNN-LSTM Model for Traffic Speed Prediction." In *2020 IEEE 91st Vehicular Technology Conference (VTC2020-Spring)*, 1-5.
- Chen, Kusano, and Gabler. 2015. 'Driver Behavior During Overtaking Maneuvers from the 100-Car Naturalistic Driving Study', *Traffic Inj Prev*, 16 Suppl 2: S176-81.

- Chen, Shi, Wong, and Yu. 2020a. 'Predicting lane-changing risk level based on vehicles' space-series features: A pre-emptive learning approach', *Transportation Research Part C: Emerging Technologies*, 116.
- Chen, Zhang, Luo, Xie, and Wan. 2020b. 'Driving Maneuvers Prediction Based Autonomous Driving Control by Deep Monte Carlo Tree Search', *IEEE Transactions on Vehicular Technology*, 69: 7146-58.
- Coifman, and Li. 2017. 'A critical evaluation of the Next Generation Simulation (NGSIM) vehicle trajectory dataset', *Transportation Research Part B: Methodological*, 105: 362-77.
- David, and Söffker. 2023. 'A review on machine learning-based models for lane-changing behavior prediction and recognition', *Frontiers in Future Transportation*, 4.
- Deng, Shahabi, Demiryurek, and Zhu. 2017. "Situation Aware Multi-task Learning for Traffic Prediction." In *2017 IEEE International Conference on Data Mining (ICDM)*, 81-90.
- Ding, Abdel-Aty, Zheng, Wang, and Wang. 2023. "Traffic flow clustering framework using drone video trajectories to identify surrogate safety measures." In, arXiv:2303.16651.
- Doshi, and Trivedi. 2008. 'A Comparative Exploration of Eye Gaze and Head Motion Cues for Lane Change Intent Prediction', *2008 IEEE Intelligent Vehicles Symposium, Vols 1-3*: 1180-85.
- Doshi, and Trivedi. 2009. 'On the Roles of Eye Gaze and Head Dynamics in Predicting Driver's Intent to Change Lanes', *IEEE Transactions on Intelligent Transportation Systems*, 10: 453-62.
- Gan, Li, Zhou, and Tang. 2021. 'Temporal convolutional networks interval prediction model for wind speed forecasting', *Electric Power Systems Research*, 191.
- Gao, Murphey, Yi, and Zhu. 2020. 'A data-driven lane-changing behavior detection system based on sequence learning', *Transportmetrica B: Transport Dynamics*, 10: 831-48.
- Gao, Murphey, and Zhu. 2018. 'Multivariate time series prediction of lane changing behavior using deep neural network', *Applied Intelligence*, 48: 3523-37.
- Gao, Yi, and Murphey. 2021. 'Joint learning of video images and physiological signals for lane-changing behavior prediction', *Transportmetrica A: Transport Science*, 18: 1234-53.
- Gidado, Chiroma, Aljojo, Abubakar, Popoola, and Al-Garadi. 2020. 'A Survey on Deep Learning for Steering Angle Prediction in Autonomous Vehicles', *IEEE Access*, 8: 163797-817.
- Gu, Abdel-Aty, Xiang, Cai, and Yuan. 2019. 'Utilizing UAV video data for in-depth analysis of drivers' crash risk at interchange merging areas', *Accid Anal Prev*, 123: 159-69.
- Guo, and Yuan. 2020. 'Short-term traffic speed forecasting based on graph attention temporal convolutional networks', *Neurocomputing*, 410: 387-93.
- Guo, Zhang, Wang, Sun, and Li. 2021. 'Driver lane change intention recognition in the connected environment', *Physica A: Statistical Mechanics and its Applications*, 575.
- Guoqing, Li, and Zhangjun. 2010. "Driver behavior analysis based on Bayesian network and multiple classifiers." In *2010 IEEE International Conference on Intelligent Computing and Intelligent Systems*, 663-68.
- Gwon, Hur, Kim, and Seo. 2017. 'Generation of a Precise and Efficient Lane-Level Road Map for Intelligent Vehicle Systems', *IEEE Transactions on Vehicular Technology*, 66: 4517-33.
- He, Zhang, Ren, and Sun. 2016. "Deep Residual Learning for Image Recognition." In *2016 IEEE Conference on Computer Vision and Pattern Recognition (CVPR)*, 770-78.
- Hou, Edara, and Sun. 2015. 'Situation assessment and decision making for lane change assistance using ensemble learning methods', *Expert Systems with Applications*, 42: 3875-82.
- Ijaz, and Wang. 2021. "Automatic Steering Angle and Direction Prediction for Autonomous Driving

- Using Deep Learning." In *2021 International Symposium on Computer Science and Intelligent Controls (ISCSIC)*, 280-83.
- Izquierdo, Parra, Munoz-Bulnes, Fernandez-Llorca, and Sotelo. 2017. "Vehicle trajectory and lane change prediction using ANN and SVM classifiers." In *2017 IEEE 20th International Conference on Intelligent Transportation Systems (Itsc)*, 1-6.
- Izquierdo, Quintanar, Parra, Fernandez-Llorca, and Sotelo. 2019. 'Experimental validation of lane-change intention prediction methodologies based on CNN and LSTM', *2019 IEEE Intelligent Transportation Systems Conference (Itsc)*: 3657-62.
- Jiang, Chang, Li, and Chen. 2020. 'Deep Transfer Learning Enable End-to-End Steering Angles Prediction for Self-driving Car', *2020 IEEE Intelligent Vehicles Symposium (IV)*: 405-12.
- Jo, Chu, and Sunwoo. 2012. 'Interacting Multiple Model Filter-Based Sensor Fusion of GPS With In-Vehicle Sensors for Real-Time Vehicle Positioning', *IEEE Transactions on Intelligent Transportation Systems*, 13: 329-43.
- Khelfa, Ba, and Tordeux. 2023. 'Predicting highway lane-changing maneuvers: A benchmark analysis of machine and ensemble learning algorithms', *Physica A: Statistical Mechanics and its Applications*, 612.
- Kumar, Perrollaz, Lefevre, and Laugier. 2013. 'Learning-Based Approach for Online Lane Change Intention Prediction', *2013 IEEE Intelligent Vehicles Symposium (IV)*: 797-802.
- Lefèvre, Vasquez, and Laugier. 2014. 'A survey on motion prediction and risk assessment for intelligent vehicles', *ROBOMECH journal*, 1.
- Li, AbuFarha, Liu, Cheng, and Gall. 2020. 'MS-TCN++: Multi-Stage Temporal Convolutional Network for Action Segmentation', *IEEE Trans Pattern Anal Mach Intell*, PP.
- Li, Jiang, Chen, and Qian. 2022a. 'Multi-step-ahead wind speed forecasting based on a hybrid decomposition method and temporal convolutional networks', *Energy*, 238.
- Li, Li, Wang, Chen, and Wu. 2023. 'Forecasting carbon prices based on real-time decomposition and causal temporal convolutional networks', *Applied Energy*, 331.
- Li, Wang, Xu, and Wang. 2016. 'Lane changing intention recognition based on speech recognition models', *Transportation Research Part C: Emerging Technologies*, 69: 497-514.
- Li, Yang, Pan, and Ma. 2022b. 'Analysing and modelling of discretionary lane change duration considering driver heterogeneity', *Transportmetrica B: Transport Dynamics*, 11: 343-60.
- Li, Zhao, Xu, Wang, Chen, and Dai. 2021. 'Lane-Change Intention Inference Based on RNN for Autonomous Driving on Highways', *IEEE Transactions on Vehicular Technology*, 70: 5499-510.
- Liu, and Pentland. 1997. 'Towards real-time recognition of driver intentions', *IEEE Conference on Intelligent Transportation Systems*: 236-41.
- Liu, Wang, Han, Shou, Tiwari, and Hansen. 2022. 'Vision-Cloud Data Fusion for ADAS: A Lane Change Prediction Case Study', *IEEE Transactions on Intelligent Vehicles*, 7: 210-20.
- Long, Shelhamer, and Darrell. 2015. "Fully convolutional networks for semantic segmentation." In *2015 IEEE Conference on Computer Vision and Pattern Recognition (CVPR)*, 3431-40.
- Ma, Zhao, Yi, Chen, Hong, and Chi. 2018. "Modeling Task Relationships in Multi-task Learning with Multi-gate Mixture-of-Experts." In *Proceedings of the 24th ACM SIGKDD International Conference on Knowledge Discovery & Data Mining*, 1930-39.
- Mahajan, Katrakazas, and Antoniou. 2020. 'Prediction of Lane-Changing Maneuvers with Automatic Labeling and Deep Learning', *Transportation Research Record: Journal of the Transportation Research Board*, 2674: 336-47.

- McCall, Wipf, Trivedi, and Rao. 2007. 'Lane Change Intent Analysis Using Robust Operators and Sparse Bayesian Learning', *IEEE Transactions on Intelligent Transportation Systems*, 8: 431-40.
- Morris, Doshi, and Trivedi. 2011. 'Lane Change Intent Prediction for Driver Assistance: On-Road Design and Evaluation', *2011 IEEE Intelligent Vehicles Symposium (IV)*: 895-901.
- Ng, Susilawati, Kamal, and Chew. 2020. 'Development of a binary logistic lane change model and its validation using empirical freeway data', *Transportmetrica B: Transport Dynamics*, 8: 49-71.
- Pan, Zhang, Zhang, Ge, Gao, Yang, and Xu. 2022. 'Lane-change intention prediction using eye-tracking technology: A systematic review', *Appl Ergon*, 103: 103775.
- Park, Jang, Lee, and Yeo. 2015. 'Logistic regression model for discretionary lane changing under congested traffic', *Transportmetrica A: Transport Science*, 11: 333-44.
- Peng, Wang, Fu, and Yuan. 2020. 'Extraction of parameters for lane change intention based on driver's gaze transfer characteristics', *Safety Science*, 126.
- Polychronopoulos, Tsogas, Amditis, and Andreone. 2007. 'Sensor Fusion for Predicting Vehicles' Path for Collision Avoidance Systems', *IEEE Transactions on Intelligent Transportation Systems*, 8: 549-62.
- Qin, Huang, Yu, Wu, Tao, and Liu. 2023. 'Geological information prediction for shield machine using an enhanced multi-head self-attention convolution neural network with two-stage feature extraction', *Geoscience Frontiers*, 14.
- Ran. 2021. 'Association Between Immediacy of Citations and Altimetrics in COVID-19 Research by Artificial Neural Networks', *Disaster Med Public Health Prep*, 17: e36.
- Ren, Wang, and Xia. 2023. 'Deep learning coupled model based on TCN-LSTM for particulate matter concentration prediction', *Atmospheric Pollution Research*, 14.
- Ruder. 2017. 'An Overview of Multi-Task Learning in Deep Neural Networks', *arXiv:1706.05098*.
- Ruina, Fang, Jianqiang, Shichun, and Keqiang. 2013. "Analysis of Chinese driver's lane change characteristic based on real vehicle tests in highway." In *16th International IEEE Conference on Intelligent Transportation Systems (ITSC 2013)*, 1917-22.
- Schmidt, Beggiato, Hoffmann, and Krems. 2014. 'A mathematical model for predicting lane changes using the steering wheel angle', *J Safety Res*, 49: 85-90.
- Sheng, Xu, Xue, and Li. 2022. 'Graph-Based Spatial-Temporal Convolutional Network for Vehicle Trajectory Prediction in Autonomous Driving', *IEEE Transactions on Intelligent Transportation Systems*, 23: 17654-65.
- Sheu, and Ritchie. 2001. 'Stochastic modeling and real-time prediction of vehicular lane-changing behavior', *Transportation Research Part B-Methodological*, 35: 695-716.
- Shi, and Zhang. 2021. 'An improved learning-based LSTM approach for lane change intention prediction subject to imbalanced data', *Transportation Research Part C: Emerging Technologies*, 133.
- Song, Peng, Yang, Wei, Wang, and Wang. 2022. "A Novel Wind Power Prediction Approach for Extreme Wind Conditions Based on TCN-LSTM and Transfer Learning." In *2022 IEEE/IAS Industrial and Commercial Power System Asia (I&CPS Asia)*, 1410-15.
- Standley, Zamir, Chen, Guibas, Malik, and Savarese. 2020. "Which Tasks Should Be Learned Together in Multi-task Learning?" In *Proceedings of the 37th International Conference on Machine Learning*, edited by Daumé Hal, III and Singh Aarti, 9120--32. Proceedings of Machine Learning Research: PMLR.
- van den Oord, Dieleman, Zen, Simonyan, Vinyals, Graves, Kalchbrenner, Senior, and Kavukcuoglu. 2016. "WaveNet: A Generative Model for Raw Audio." In, *arXiv:1609.03499*.

- Wang, Li, and Li. 2014. 'Investigation of Discretionary Lane-Change Characteristics Using Next-Generation Simulation Data Sets', *Journal of Intelligent Transportation Systems*, 18: 246-53.
- Wang, Qie, Yang, Liu, Xiang, and Huang. 2022. 'An Intelligent Lane-Changing Behavior Prediction and Decision-Making Strategy for an Autonomous Vehicle', *IEEE Transactions on Industrial Electronics*, 69: 2927-37.
- Wang, Wang, Bi, Weng, and Yan. 2016. 'Modeling the probability of freeway lane-changing collision occurrence considering intervehicle interaction', *Traffic Inj Prev*, 17: 181-7.
- Xing, Lv, Wang, Cao, and Velenis. 2020. 'An ensemble deep learning approach for driver lane change intention inference', *Transportation Research Part C: Emerging Technologies*, 115.
- Xu, Liu, Ou, and Song. 2012. 'Dynamic Modeling of Driver Control Strategy of Lane-Change Behavior and Trajectory Planning for Collision Prediction', *IEEE Transactions on Intelligent Transportation Systems*, 13: 1138-55.
- Xu, Wen, Zhao, Liu, and Zhang. 2019. 'The Hybrid Model for Lane-Changing Detection at Freeway Off-Ramps Using Naturalistic Driving Trajectories', *IEEE Access*, 7: 103716-26.
- Xu, Zhang, Cheng, and Xu. 2020. 'MTLM: a multi-task learning model for travel time estimation', *GeoInformatica*, 26: 379-95.
- Xu, Zhang, Wu, Qi, and Han. 2021. 'Recognition of lane-changing behaviour with machine learning methods at freeway off-ramps', *Physica A: Statistical Mechanics and its Applications*, 567.
- Yang, Wang, and Quddus. 2019. 'Examining lane change gap acceptance, duration and impact using naturalistic driving data', *Transportation Research Part C: Emerging Technologies*, 104: 317-31.
- Yang, Wu, Sun, Chen, Zhai, and Fu. 2021. 'Freeway accident detection and classification based on the multi-vehicle trajectory data and deep learning model', *Transportation Research Part C: Emerging Technologies*, 130.
- Yating, Wu, Qiongbina, Fenghuang, and Qinqin. 2021. 'Fault Diagnosis for Power Converters Based on Optimized Temporal Convolutional Network', *IEEE Transactions on Instrumentation and Measurement*, 70: 1-10.
- Yeon, Min, Shin, Sunwoo, and Han. 2019. 'Ego-Vehicle Speed Prediction Using a Long Short-Term Memory Based Recurrent Neural Network', *International Journal of Automotive Technology*, 20: 713-22.
- Zhang, Lee, Abdel-Aty, Zheng, and Xiao. 2023. 'Enhanced index of risk assessment of lane change on expressway weaving segments: A case study of an expressway in China', *Accid Anal Prev*, 180: 106909.
- Zhang, Sun, Qi, and Sun. 2019. 'Simultaneous modeling of car-following and lane-changing behaviors using deep learning', *Transportation Research Part C: Emerging Technologies*, 104: 287-304.
- Zhang, and Yang. 2018. 'An overview of multi-task learning', *National Science Review*, 5: 30-43.
- Zhang, Yang, Zhou, Wang, and Ouyang. 2021. 'Multi-city traffic flow forecasting via multi-task learning', *Applied Intelligence*, 51: 6895-913.
- Zhao, Gao, Bai, Wang, and Lu. 2019a. 'Traffic Speed Prediction Under Non-Recurrent Congestion: Based on LSTM Method and BeiDou Navigation Satellite System Data', *IEEE Intelligent Transportation Systems Magazine*, 11: 70-81.
- Zhao, Gao, Yang, Li, Feng, Qin, and Bai. 2019b. 'Truck Traffic Speed Prediction Under Non-Recurrent Congestion: Based on Optimized Deep Learning Algorithms and GPS Data', *IEEE Access*, 7: 9116-27.

- Zheng, Abdel-Aty, Yue, Abdelraouf, Wang, and Mahmoud. 2022. "CitySim: A Drone-Based Vehicle Trajectory Dataset for Safety Oriented Research and Digital Twins." In, arXiv:2208.11036.
- Zheng, and Hansen. 2017. 'Lane-Change Detection From Steering Signal Using Spectral Segmentation and Learning-Based Classification', *IEEE Transactions on Intelligent Vehicles*, 2: 14-24.
- Zheng, Suzuki, and Fujita. 2014. 'Predicting driver's lane-changing decisions using a neural network model', *Simulation Modelling Practice and Theory*, 42: 73-83.